Enhanced backscattering in a converging-beam configuration

Aristide Dogariu and Glenn D. Boreman

Center for Research and Education in Lasers and Optics, University of Central Florida, Orlando, Florida 32816

Received July 17, 1996

Enhanced backscattering (EBS) is investigated for a converging-beam geometry. We find that the functional form of the enhanced backscattering cone is preserved under a change of variables that involves the focal length of the lens and the lens-to-sample distance. In absolute terms, the effect of the lens is that the EBS enhancement cone is lowered in magnitude and narrowed in angle. The experimental data show good agreement with the theory presented, even for tightly focused beams, as long as the illuminated area is larger than the transport mean free path for the random medium. © 1996 Optical Society of America

It is well known that the intensity of light multiply scattered from random media is enhanced in the backward direction. The phenomenon of enhanced backscattering (EBS) has been described as a manifestation of the weak localization of light,[1] and effects of various experimental parameters such as absorption, finite size, interface reflectivity, Faraday rotation, and finite coherence length were studied.[2–7] These reports treated a plane-wave incidence, and, to the best of our knowledge, there have been no studies of the effect of a converging-beam illumination geometry. In this Letter we investigate the effect of the converging-beam configuration on the line shape and magnitude of the EBS peak, and possible applications of EBS are suggested.

We consider a volume-scattering medium placed at a distance d behind a lens with a focal length $F \geq d$, as shown in Fig. 1. In this configuration, photons are injected over the illuminating area S and collected over a larger receiving area S_0. Two particular scattering centers are located at $\mathbf{r}_l$ and $\mathbf{r}_m$ in the random medium and are separated by a projected distance $\rho = |\mathbf{r}_l - \mathbf{r}_m|_{\|}$ measured along the interface. Waves with the initial and the final wave vectors $\mathbf{k}_i$ and $\mathbf{k}_f$, respectively, that have $\mathbf{r}_l$ and $\mathbf{r}_m$ as the end points of their trajectories and that have traveled through the same scattering centers but in reverse order, will experience a phase difference $\Delta\phi \propto (\mathbf{k}_i + \mathbf{k}_f)(\mathbf{r}_l - \mathbf{r}_m)$, giving rise to the phenomenon of enhanced backscattering. A rigorous analysis can be developed on the basis of complex scattering amplitudes A_{lm} of waves incident at $\mathbf{r}_l$ and emergent at $\mathbf{r}_m$.[8] The far-field intensity of the reflected wave is a contribution of three terms:

$$I = I_0 + I_{\text{fluc}} + I_{\text{ebs}}, \tag{1}$$

where the first term, I_0, is the background intensity:

$$I_0(\mathbf{k}_i, \mathbf{k}_f) = \sum_{l,m \in S_0} |A_{lm}|^2, \tag{2}$$

the second, I_{fluc}, represents the speckle fluctuations:

$$I_{\text{fluc}}(\mathbf{k}_i, \mathbf{k}_f) = \sum_{(l,m)\in S_0 \neq (l',m')\in S_0} A_{lm}{}^* A_{l'm'} \times \exp[ik_i(\mathbf{r}_l - \mathbf{r}_{l'})]\exp[i\mathbf{k}_f(\mathbf{r}_m - \mathbf{r}_{m'})], \tag{3}$$

and the third term, I_{ebs}, expresses contributions from the time-reversed scattering paths:

$$I_{\text{ebs}}(k_i, \mathbf{k}_f) = \sum_{l,m \in S} |A_{lm}|^2 \cos(\mathbf{k}_i + \mathbf{k}_f)(\mathbf{r}_l - \mathbf{r}_m). \tag{4}$$

The summation in Eq. (4) includes only those paths for which the projection $|\mathbf{r}_l - \mathbf{r}_m|_{\|}$ along the interface is included in the illuminated area S.

When an ensemble average is taken over different realizations of the scattering medium, the speckle term of Eq. (3) is zero, and the angular dependence of the reflected wave intensity becomes

$$I(\mathbf{k}_i, \mathbf{k}_f) = \sum_{l,m \in S_0 - S} P_{l,m} + \sum_{l,m \in S} P_{l,m} + \sum_{l,m \in S} P_{l,m} \cos(\mathbf{k}_i + \mathbf{k}_f)(\mathbf{r}_l - \mathbf{r}_m). \tag{5}$$

The squared modulus of the complex scattering amplitude $|A_{lm}|^2 = P_{l,m}$ represents the probability that a photon injected at point l is emitted at point m. The first term of Eq. (5) refers to scattering paths that end outside the illuminated area and, therefore, constitute time-reversed paired paths. The second and the third terms in Eq. (5) constitute the ladder and the cyclical contributions, respectively, of a classical EBS description over area S.[1] The first term can then be regarded as an additional ladder term. In a dense medium with a large number of possible multiple-scattering channels, the three terms depicted in Eq. (5) are proportional to the area over which they are evaluated, and, in a continuum limit, the angular dependence of the backscattered intensity becomes

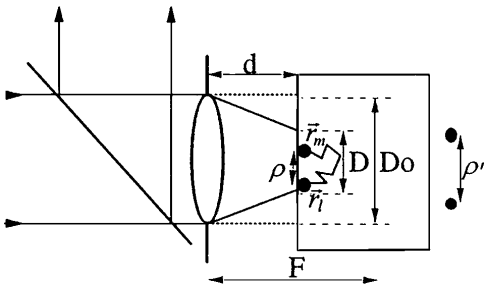

Fig. 1. EBS experiment in a converging-beam configuration.

0146-9592/96/211718-03$10.00/0

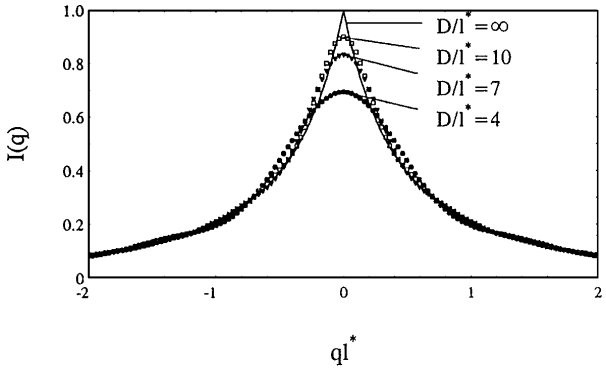

Fig. 2. Calculated EBS line shapes for various diameters of the illuminated area and for the case of infinitely extended plane-wave illumination.

$$I(q) = 1 + \left(\frac{F-d}{F}\right)^2 \int_0^D P(\rho)\exp(iq\rho)\rho \mathrm{d}\rho\,, \qquad (6)$$

where $\mathbf{q} = |\mathbf{k}_i + \mathbf{k}_f|$ is the momentum transfer, $P(\rho)$ is the probability-density function of the separation distance ρ, D is the diameter of the illuminated area S, and the factor in front of the integral is the ratio between the illumination and the receiving areas and accounts for the decreased contribution of paired loops.

The angular profile of the coherent enhancement is determined by the form of the probability $P(\rho)$. In a simple interpretation, the enhanced backscattering is built up by random superpositions of interference patterns generated by pairs of coherent point sources. In this respect Eq. (4) is interpreted as a superposition of randomly oriented Young interference fringes, corresponding to coherent sources separated by a distance ρ. In the converging-beam configuration the effect of the lens is to increase the apparent separation between the coherent sources. In the configuration of Fig. 1 the lens produces a virtual object separation $\rho' = \rho F/(F - d)$. Accordingly, the new shape of the EBS peak is described by

$$I(q) = 1 + \eta \int_0^{D_0(F-d/F)} P(\rho)\exp\left(iq\rho\,\frac{F}{F-d}\right)\rho \mathrm{d}\rho\,. \qquad (7)$$

The EBS shape is preserved, provided that a variable transformation $q' = \eta q$ is performed, where $\eta = 1 - d/F$. Analyzing Eq. (7), we see that the effect of the converging-beam geometry is twofold. First, the magnitude of the EBS cone is decreased by a multiplicative factor η. Second, the cone is narrowed, while its function form is preserved. This is rigorously true as long as the upper limit of the integral in Eq. (7) can be considered infinite. This requirement is inherently satisfied in a plane-wave geometry; but, in the converging-beam configuration where the illumination area is reduced, it is important to know the limit of this approximation. We investigate the effect of illumination spot size on the EBS line shape by evaluating the coherent enhancement $\int_0^D P(\rho)\exp(iq\rho)\mathrm{d}^2\rho$ for different values of the integration limit D. For the general case of anisotropic scattering, the distribution $P(\rho)$ is obtained from the transport theory[9] as a Bessel transform:

$$P(\rho) = \frac{1}{4\pi^2}\,\frac{l^*}{l}\int_0^\infty \frac{x}{1 + {}^2\!/_3 l^* x}\left(\frac{1}{1+lx} + \frac{l}{l^*} - 1\right) \times J_0(\rho x)\mathrm{d}x\,, \qquad (8)$$

where l and l^* are the elastic and the transport mean free paths, respectively. In Fig. 2 the results of a numerical integration of the EBS enhancement cone are shown for $D/l^* = 10$, 7, 4 as well as for the case of $D/l^* = \infty$. As can be seen, sensible effects that decrease the EBS magnitude with more than 10% are seen only for $D/l^* < 10$. This is caused by the suppression, in the present geometry, of the long scattering paths. These paths contribute primarily to the small-angle region of the EBS enhancement cone. Similar effects are produced when scattering paths are suppressed by absorption and finite thickness,[2,3] Faraday rotation,[5] and reduced coherence.[6] We conclude that the EBS line-shape degradation attributable to the finite size of illuminated area S becomes important only for small illuminated areas. For dense, solid random media with l^* of the order of several tens of micrometers, the ratio D/l^* is usually quite large, and the finite-size effect is negligible in comparison with the decreased-magnitude and cone-narrowing terms of Eq. (7).

Experiments have been conducted in the geometry presented in Fig. 1. The experimental apparatus[7] includes a lens with a focal length $F = 50$ mm and a translation stage that permits variation of the lens-to-sample distance $d > 10$ mm. Lens aperture D_0 determines the original diameter of the incident beam and was set to 8 mm in the present experiment. The multiple-scattering medium was a sample of Spectralon[10] material, which was rotated during the acquisition of (typically) 50 frames. We also recorded EBS in a plane-wave illumination geometry and inferred a value $l_0^* = 23$ μm for the Spectralon sample.

In Fig. 3(a) semicones of coherent enhancement are presented for various distances d. The curve labeled $d = 0$ mm corresponds to the case of plane-wave illumination. Also shown, by a continuous curve, is the theoretical dependence obtained in the diffusion approximation[9]

$$I(q) = \eta\left\{\frac{2z_0}{l^*} + \frac{1}{(1+ql^*)^2}\left[1 + \frac{1-\exp(-2qz_0)}{ql^*}\right]\right\}, \qquad (9)$$

with $q = 2\pi/\lambda\theta$ and $z_0 = 0.7104l^*$ for $\eta = 1$ and $l^* = l_0^* = 23$ μm. As can be seen, in the case of plane-wave illumination the intensity enhancement is close to the ideal factor of 2 but decreases for larger d. The same data are replotted in Fig. 3(b), with the angular variables scaled by $F/(F - d)$ and the intensity values multiplied by $F/(F - d)$. All the experimental data behave in a similar manner after scaling, showing that the functional form of the coherent-enhancement cone is not changed.

For a quantitative assessment of the present model we fitted the scattered-intensity data with the form given in Eq. (9), with η and l^* as independent fitting parameters. These results are summarized in Fig. 4.

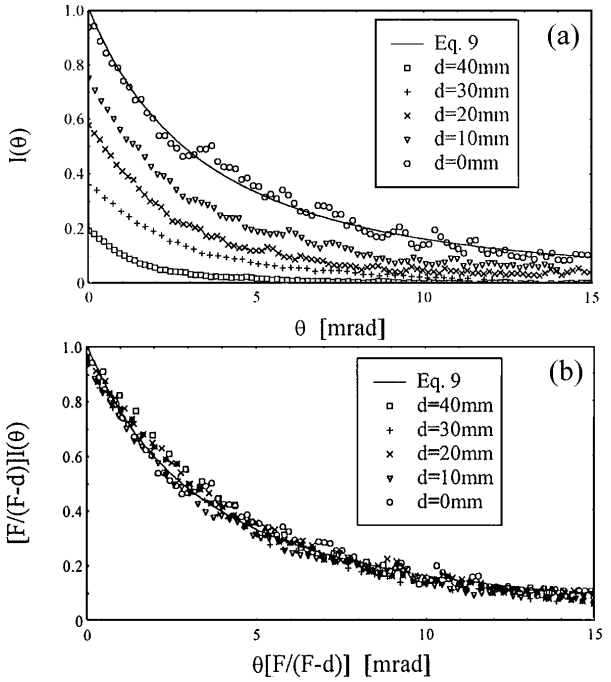

Fig. 3. (a) Coherent enhancement data corresponding to the Spectralon sample placed at various distances d behind a lens with $F = 50$ mm and (b) the same data scaled as indicated. Also shown, by the continuous curve, is the EBS shape predicted by the diffusion approximation for $l^* = l_0^* = 23\ \mu$m.

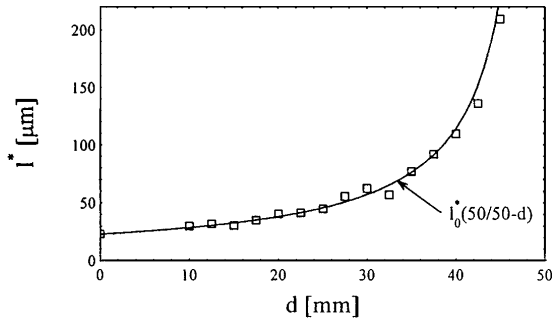

Fig. 4. Values of the apparent transport mean free path as obtained by fitting the experimental EBS cones with the theoretical dependence of Eq. (9).

The apparent transport mean free path, as inferred from the fit, varies as expected: $l^* = l_0^*[50/(50 - d)]$. This dependence is followed to $d = 45$ mm, where the illuminated area is just 0.8 mm in diameter because, even for such a small area, $D \gg l^*$.

This study adds to a more comprehensive picture of the EBS phenomenon from the viewpoint of both its theoretical and experimental descriptions. In the converging-beam geometry discussed here, photon collection is made over an area that is larger than the illuminated one, and this naturally results in a decrease of the peak magnitude. In other words, the ladder term corresponding to the incoherent background is increased compared with the cyclical term given by the time-reversed paths. We have shown that the lens effectively magnifies the scattering mean free path and, accordingly, determines the narrowing of the cone without altering its functional dependence. We have demonstrated that, for a random medium placed a distance d behind a lens, the effect of the converging-beam configuration is fully controllable and that the EBS magnitude and angular width depend on distance d. Applications of practical interest, such as range measurement and location of diffusive targets, can benefit from the present study. The converging-beam configuration described here is also potentially significant for experimental investigations of multiple-scattering effects in random media with nonlinear-optical properties because of the increased irradiance available from a focused beam.

References

1. P. Sheng, *Scattering and Localization of Classical Waves in Random Media* (World Scientific, Singapore, 1990).
2. S. Etemad, R. Thompson, and M. J. Andrejo, Phys. Rev. Lett. **59,** 1420 (1987).
3. I. Edrei and M. Kaveh, Phys. Rev. B **35,** 6461 (1987).
4. P. M. Saulnier and G. H. Watson, Opt. Lett. **17,** 946 (1992).
5. F. C. MacKintosh and S. John, Phys. Rev. B **37,** 1884 (1988).
6. M. Tomita and H. Ikari, Phys. Rev. B **43,** 3716 (1991).
7. A. Dogariu, G. D. Boreman, and M. Dogariu, Opt. Lett. **20,** 1665 (1995).
8. M. Kaveh, M. Rosenbluh, I. Edrei, and I. Freund, Phys. Rev. Lett. **57,** 2049 (1986).
9. E. Akkermans, P. E. Wolf, R. Maynard, and G. Maret, J. Phys. (Paris) **49,** 77 (1988).
10. Spectralon, a diffuse reflectance material; Labsphere, Inc., North Sutton, New Hampshire.